Thermally stimulated shrinkage forces in oriented polymers: 2. Time dependence

M. Trznadel, T. Pakula and M. Kryszewski
Centre of Molecular and Macromolecular Studies, Polish Academy of Science, Łódź, ul. Boczna 5, Poland
(Received 13 February 1984)

The four-state model proposed in a previous paper to describe thermal shrinkage in oriented polymers is solved to describe the time dependences of shrinkage forces under constant temperature conditions. The time dependences of shrinkage forces have been recorded for polycarbonate and polyethylene terephthalate at temperatures below the glass transition. It is shown that experimentally recorded time dependences of shrinkage forces can be satisfactorily fitted by dependences predicted by the model, and the comparison leads to reasonable values of activation energy and activation volume for the shrinkage process.

(Keywords: thermal shrinkage; shrinkage forces; orientation; model; amorphous polymers)

INTRODUCTION

The thermal shrinkage of polymers is a time and temperature dependent phenomenon. The time dependence can be observed as the influence of heating rate on the temperature dependence of shrinkage or as a time dependent shrinkage under constant temperature conditions[1-3].

When an oriented polymer sample is heat-treated under external conditions which make shrinkage impossible, stresses are generated which are dependent on time and temperature. In the previous paper[4] we have shown various examples of the temperature dependences of thermally stimulated shrinkage forces (*TSSF*) when the oriented sample was heated at a constant heating rate under constant length conditions[4]. The mechanism of generation of shrinkage forces and the temperature dependences were discussed and explained in terms of a four-state model. The model assumes that extended molecular subunits can undergo thermally activated transition from their oriented to unoriented states and that this transition is influenced by internal stresses exerted by the extended macromolecules on the local frozen-in configurations. This transition leads to intermediate states in which the initially frozen-in internal stresses are transduced to the surrounding matrix when the local molecular orientation is relaxed. These defrozen stresses can be detected macroscopically. The forces of shrinkage generated in this way can be relaxed by various molecular rearrangements such as intermolecular slip. The model has been shown to predict qualitatively correct temperature dependences of shrinkage forces in oriented amorphous polycarbonate.

In this paper we use this model, with some simplifying assumptions, to describe the time dependences of shrinkage forces under constant temperature conditions. The calculated results are compared with experimental data obtained for oriented amorphous polycarbonate and poly(ethylene terephthalate) samples.

THE MODEL

The model was described in detail in the previous paper[4]. Graphical representation of a single model element is shown in *Figure 1*. It consists of two springs: S_1 connected in parallel with a two-site element and S_2 connected in series with another two-site element.

Molecular interpretation of this model element assumes that spring S_1 is related to the chain elasticity, and when extended (in site 2) it represents an oriented configuration of a molecular subunit; in site 1 it represents a relaxed chain orientation. Spring S_2 represents an elastic junction of the subunit with the matrix and its extension can be relaxed by overcoming the potential barrier between sites 3 and 4, for example as a result of intermolecular slip.

At constant length the whole element can assume four states depending on whether spring S_1 assumes site 1 or 2 and on whether spring S_2 assumes site 3 or 4. The local situation in oriented polymer can be represented by a state in which spring S_1 is in site 2 and spring S_2 is in site 3 (state A). By a single jump in one of the two-site elements the model can be transformed from state A to two other states. When the jump takes place from site 2 to 1, state B is obtained. The jump from state 3 to 4 leads to the less probable state D. States B and D can both be transformed to state C in which sites 1 and 4 are occupied. A simple analysis of the model shows that the initial state A, being externally relaxed is internally stressed and can be transformed to the fully relaxed state C through the intermediate state B or D which exert external stresses when the length of the element is kept constant.

An assembly of such model elements connected with each other is taken to be a model of an oriented polymer. Its behaviour is defined by the probabilities of jumps

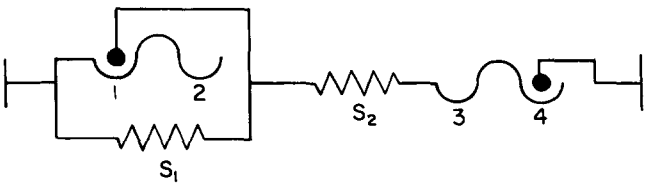

Figure 1 Representation of the four state model

0032-3861/85/071019-06$03.00

between sites in single model elements. These probabilities depend on the type of connection between the elements, on the initial state of the model and on external conditions. It is further assumed that the initial state of such a model consists of elements most of which are in state A and that the length of the model is kept constant.

The heights of potential barriers between the sites of two-site elements are assumed to be defined by the Helmholtz free energy difference related to excitation of the local frozen-in molecular configuration. However, the probabilities of transitions between sites are influenced by mechanical energy related to local stresses represented in the model by springs S_1 and S_2.

In such a case, in the model built up of elements connected in parallel the probabilities of transition can be given by

$$K_{AB}=K_{BA}=K_{BC}=K_{DA}=A\exp\left(-\frac{\Delta F-E}{kT}\right) \quad (1a)$$

$$K_{CB}=K_{AD}=K_{CD}=A\exp\left(-\frac{\Delta F}{kT}\right) \quad (1b)$$

$$K_{DC}=A\exp\left(-\frac{\Delta F-2E}{kT}\right) \quad (1c)$$

where K_{IJ} denote probabilities of transition from state I to state J, A is a constant, ΔF is the Helmholz free energy barrier for the local structural rearrangement, and E is the mechanical energy influencing the effective height of the barrier and given by[5]:

$$E=\sigma_0 V\Delta\varepsilon \quad (2)$$

where σ_0 is the local stress, V is the activation volume and $\Delta\varepsilon$ is the strain change related to the rearrangement. These simplified parameters are valid under the assumption that the Helmholz free energy contour is described by the non-zero strain resistance $d\Delta F/d\varepsilon$ at the stable equilibrium position of all sites in the model. As a result of this assumption only two positions at the bottom of sites can be occupied in the two-site element unless the element is excited by a cooperative action of both stresses exerted by springs and thermal free energy fluctuation.

In the above case of the parallel model the probabilities are constant at constant temperature.

In the case of the series connection of elements the probabilities change with the change of populations of states B and D which influences the mechanical energy component

$$K_{BA}=K_{BC}=K_{AD}=K_{CD}=A\exp\left(-\frac{\Delta F-E_1}{kT}\right) \quad (3a)$$

$$K_{DA}=K_{CB}=A\exp\left(-\frac{\Delta F+E_1}{kT}\right) \quad (3b)$$

$$K_{AB}=K_{DC}=A\exp\left(-\frac{\Delta F-E+E_1}{kT}\right) \quad (3c)$$

where E_1 is the mechanical energy component influenced by the populations n_b and n_d of states B and D respectively and can be expressed by

$$E_1=(n_b-n_d)\sigma_0 V\Delta\varepsilon \quad (4)$$

The probabilities related to both models were determined under the assumption that the quantities describing transitions between sites 1 and 2, and 3 and 4 are identical.

As can be seen from the above expressions, the probability that the transition from state A to C proceeds via state D is much smaller than the transition through state B, especially in the case of the parallel model. Therefore in what follows we will consider only a transition of the type

$$A\leftrightarrow B\leftrightarrow C$$

which can be described by a set of differential equations

$$\frac{dn_a}{dt}=-K_{AB}n_a+K_{BA}n_b \quad (5a)$$

$$\frac{dn_b}{dt}=K_{AB}n_a-(K_{BA}+K_{BC})n_b+K_{CB}n_c \quad (5b)$$

$$\frac{dn_c}{dt}=K_{BC}n_b-K_{CB}n_c \quad (5c)$$

and the condition that

$$n_a+n_b+n_c=1 \quad (6)$$

where n_a, n_b and n_c are populations of states A, B and C respectively.

These equations are relatively easy to solve in the case of the parallel model for which K_{IJ} are constant. This leads to

$$n_a=C_1\exp(a_1t)+C_2\exp(a_2t)+C_3 \quad (7a)$$

$$n_b=C_4\exp(a_1t)+C_5\exp(a_2t)+C_6 \quad (7b)$$

$$n_c=1-n_a-n_b \quad (7c)$$

(the solution reported in many mathematics textbooks, e.g. ref. 6) where constants C_1 and a_1, a_2 depend on probabilities K_{IJ}. For the series model, equations (5) can be solved numerically.

In both cases of the parallel and series connection of elements in the model, the external stress exerted by the model is proportional to the population of elements in state B. Therefore the time dependence of n_b will be regarded as describing the time dependence of shrinkage forces predicted by the model.

Examples of time dependences of n_b calculated according to both parallel and series models for some arbitrary parameters and conditions are shown in *Figure 2* and *Figure 3*. The influence of the mechanical energy component on the dependence of n_b vs. time predicted by the parallel model is illustrated in *Figure 2*. *Figure 3* shows the effect of temperature as predicted by the parallel and series models. These examples show that both models predict qualitatively similar dependences. Generally, it is seen that the models predict time dependences of shrinkage forces with maxima whose position on the time scale, depend on the contribution of the mechanical energy component and temperature.

EXPERIMENTAL

The time dependences of shrinkage forces were recorded

using the apparatus described in the previous paper[4]. The oriented polymer sample was clamped at room temperature and quickly immersed in an oil bath thermostatically controlled at an elevated temperature. From this moment on the force of shrinkage was measured. The length of the sample was constant during the whole experiment.

Two polymers were studied: polycarbonate Macrolon 2408 and commercial films of poly(ethylene terephthalate). Amorphous, unoriented films of polycarbonate 0.6 mm thick were obtained by press moulding at the temperature of 240°C. Films were oriented by cold drawing (at room temperature) with the drawing rate of 1 cm/min. Drawn films had the natural draw ratio of about 2 and they were 0.3 mm thick. Amorphous poly(ethylene terephthalate) films were drawn at room temperature at a constant drawing rate of 0.5 cm/min to the natural draw ratio $\lambda=4$. Drawn films had the thickness of 0.15 mm.

The time dependences of the shrinkage forces were recorded at temperature not much higher than room temperature and below the glass transition temperatures for both polymers.

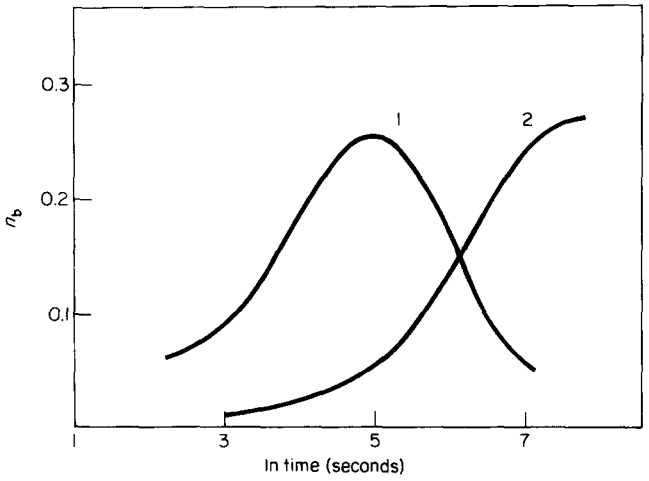

Figure 2 Time dependences of population n_b of states B predicted by the parallel model for various contributions of the mechanical energy component: (1) $E=3.7\,kT_0$, (2) $E=1.1\,kT_0$; $T_0=273$ K, $\Delta F=73\,kT_0$

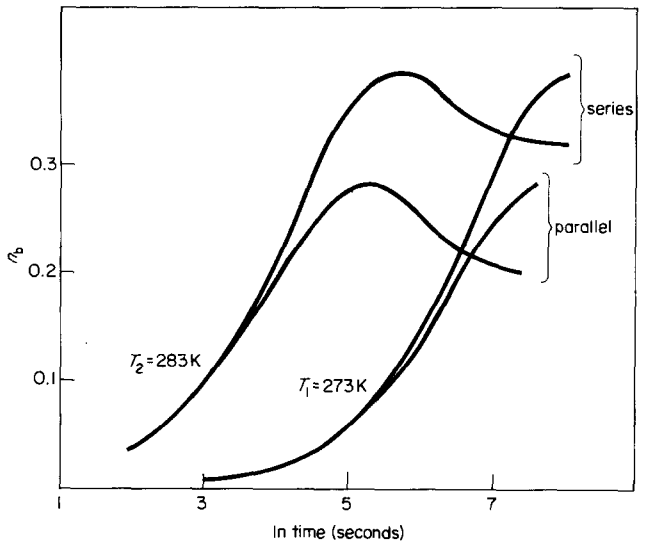

Figure 3 Time dependences of populations n_b predicted by the parallel and series models for two different temperatures ($\Delta F=73\,kT_0$, $E=1.1\,kT_0$)

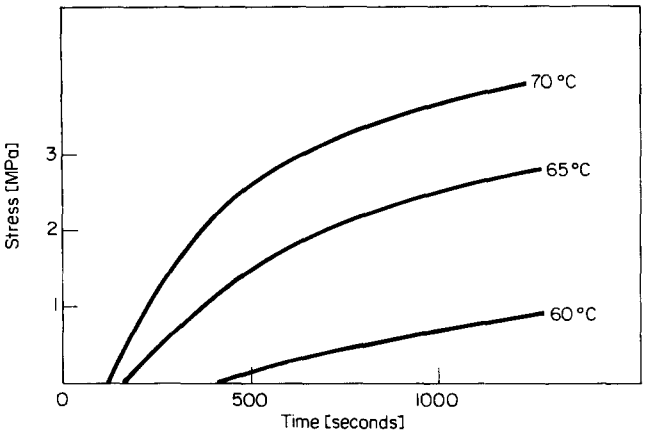

Figure 4 Shrinkage stresses vs. time at various temperatures for oriented polycarbonate

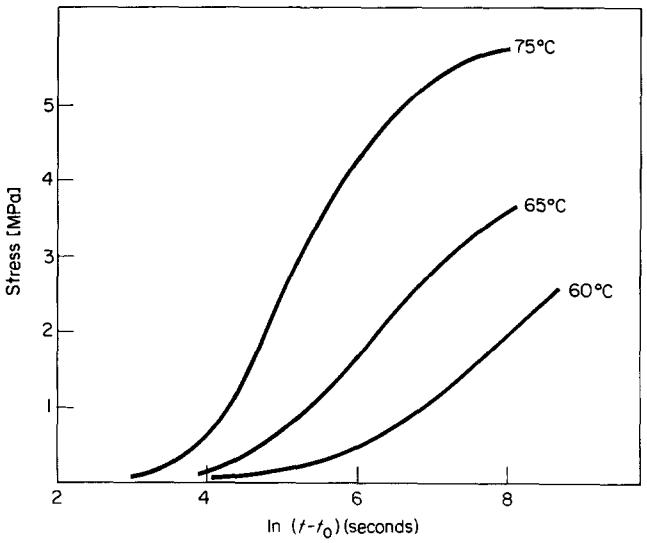

Figure 5 Shrinkage stresses in polycarbonate vs. $\ln(t-t_0)$ at various temperatures

RESULTS AND DISCUSSION

Figure 4 shows the time dependences of shrinkage stresses generated in samples of polycarbonate. An induction time, at which the non-zero stress appears, is observed in all cases. After the induction period the stress increases quickly slowing down at longer times but it does not reach any constant or maximal value in the time interval of the experiments performed. Considering that the dependences presented in *Figure 4* were recorded well below the glass transition temperature of polycarbonate, it is quite likely that only the initial stages of the possible time dependences predicted by the model described in the preceding section were observed.

This becomes all the more likely when the experimental values of shrinkage stress are plotted (*Figure 5*) as a function of $\ln(t-t_0)$ (t_0 is the induction time) and compared with dependences of n_b vs. $\ln t$ predicted by the models (*Figure 3*). It can be seen that the shape of shrinkage force changes agrees well with the shape of the time dependences of n_b described by the models. It follows from this qualitative comparison that the possibility of experimental observation of any maximum of shrinkage forces requires experiments performed over ten times longer periods or at higher temperatures. We did not perform any experiments at higher temperatures because

of the considerable influence of the effects of heat transfer from the immersion liquid to the sample, which disturbs the shapes of shrinkage force changes when the height of the temperature jump is too high.

An example of the time dependences of shrinkage forces recorded at 110°C is shown in *Figure 6*. In this case the reference temperature for the temperature jump was 90°C at which the sample of oriented polycarbonate was annealed with free ends for 5 min just before the experiment. This result shows that at a temperature close to glass transition, a time dependence of shrinkage very similar to that predicted by the model (compare *Figure 2*), can be recorded in a reasonable experimental time period.

In the case of poly(ethylene terephthalate) the situation is additionally complicated by crystallization taking place at temperatures close to the glass transition. The shrinkage forces recorded in this polymer at various temperatures below the glass transition are plotted in *Figure 7* as a function of $\ln(t-t_0)$. As in the case of polycarbonate in experiment performed at lower temperatures the changes of shrinkage forces are qualitatively the same as those predicted by the initial parts of the calculated dependences shown in *Figure 3*. However, at temperatures above 60°C, i.e. close to the glass transition at which crystallization of oriented samples of poly(ethylene terephathalate) is clearly observed[7], the trace of shrinkage force is considerably disturbed by the delayed heat transfer from the immersion liquid to the sample at the beginning of the experiment and by the effect of crystallization at longer times.

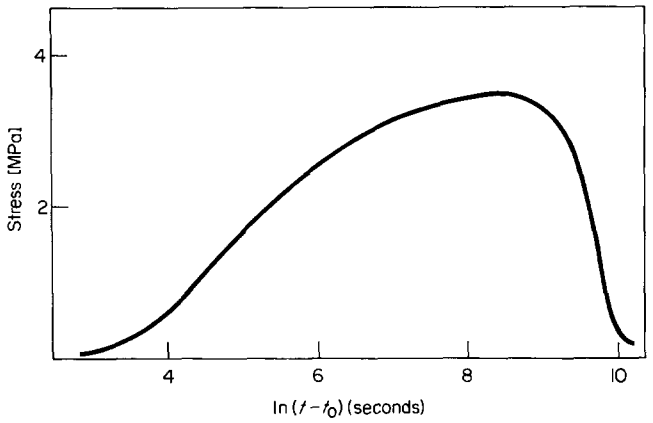

Figure 6 Time dependence of shrinkage stresses in polycarbonate at 110°C after a temperature jump from 90°C

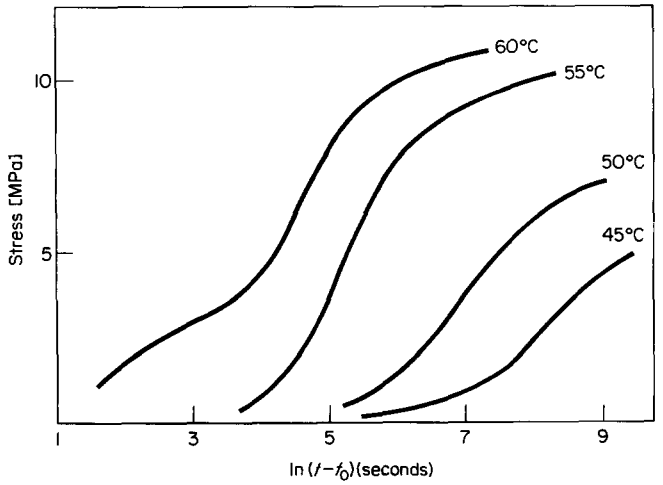

Figure 7 Shrinkage stresses in poly(ethylene terephthalate) vs. $\ln(t-t_0)$ at various temperatures

Table 1 Induction time of appearance of shrinkage forces under constant temperature conditions

	Induction time (s)	
T (°C)	PC	PET
45	5600	144
50	2700	90
55	1300	22
60	405	7
65	165	–
70	120	–

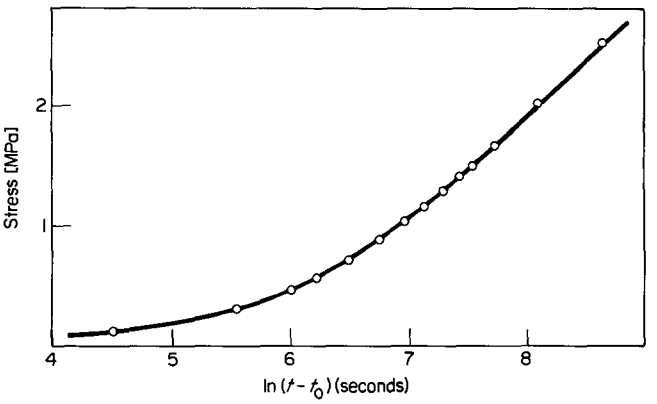

Figure 8 Fit between experimental data of shrinkage forces in polycarbonate at 60°C and the equation related to initial behaviour of the series model

The temperature dependent induction time was observed also for poly(ethylene terephthalate). The values of the induction time for both polymers are given in *Table 1*.

The temperature dependent induction time was observed also for poly(ethylene terephthalate). The values of the induction time for both polymers are given in *Table 1*.

Because of the effects described above and because of the limited time period of the experiments performed, a comparison of the measured and calculated dependences over a wide temperature interval is not possible. A direct comparison can however be performed between the experimental results obtained and the initial stages of the transition described by the model.

The initial stage of the reaction considered in the model can be described by the transition A→B for which equation (5b) reduces to

$$\frac{dn_b}{dt}=(1-n_b)K_{AB} \tag{8}$$

Taking into account that the external stress σ in the model is proportional to n_b, we fitted the above equation to the experimental data. An example is shown in *Figure 8* in which the experimental shrinkage stress values obtained for the polycarbonate at 60°C are fitted by the equation

$$\frac{d\sigma}{dt}=(1400-2.9\cdot10^{-4}\sigma)\exp(-6\cdot10^{-5}\sigma) \tag{9}$$

which is equivalent to equation (8) when applied to the series model.

The good agreement between experimental data and

the numerically fitted curve as well as the fact that both models predict similar dependences at the initial stages of the considered transition rationalizes application of both models to the evaluation of activation energy and activation volume for the molecular processes related to generation of shrinkage forces.

For the parallel model, equation (8) can be solved and the solution, when expressed in the linearized form, is given by

$$\ln(S-\sigma) = -K_{AB}t + \ln S \qquad (10)$$

where S is a constant. Plotting $\ln(S-\sigma)$ vs. t we can determine values of K_{AB} from the slope of the plot as illustrated in *Figure 9*. Having determined the values of K_{AB} for various temperatures and plotting $\ln(K_{AB})$ vs. $1/T$ we can determine the activation energy $\Delta G = \Delta F - E$ of the observed process. An example of such a plot for polycarbonate is shown in *Figure 10*. Using this procedure we determined the values of ΔG for both polymers studied:

$\Delta G = 46$ kcal mol^{-1} for PC

$\Delta G = 30$ kcal mol^{-1} for PET

For the series model the probability K_{AB} given by equation (3c) depends on the external stress σ and it can be expressed in the form

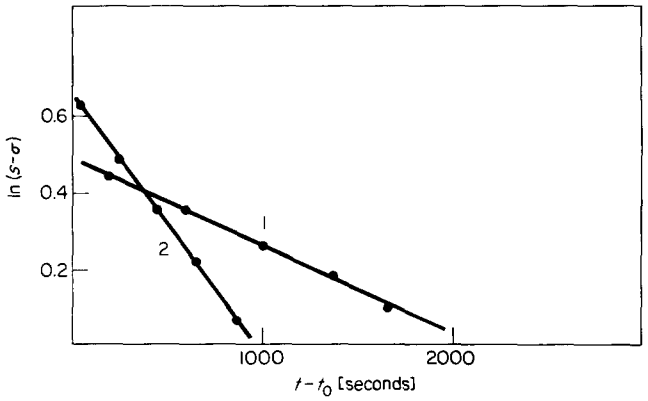

Figure 9 Plots of $\ln(S-\sigma)$ vs. t for polycarbonate samples at two temperatures, (1) $T = 55$°C, $S = 1.63$ MPa; (2) $T = 60$°C, $S = 1.95$ MPa

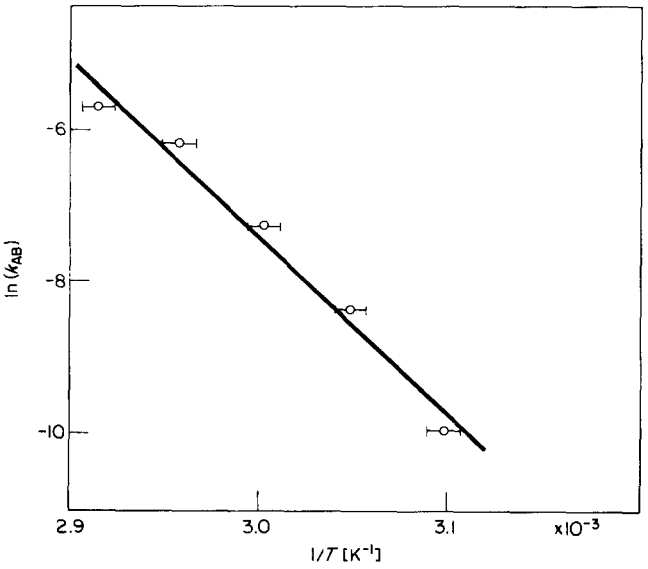

Figure 10 Plot of K_{AB} vs. $1/T$ for polycarbonate samples

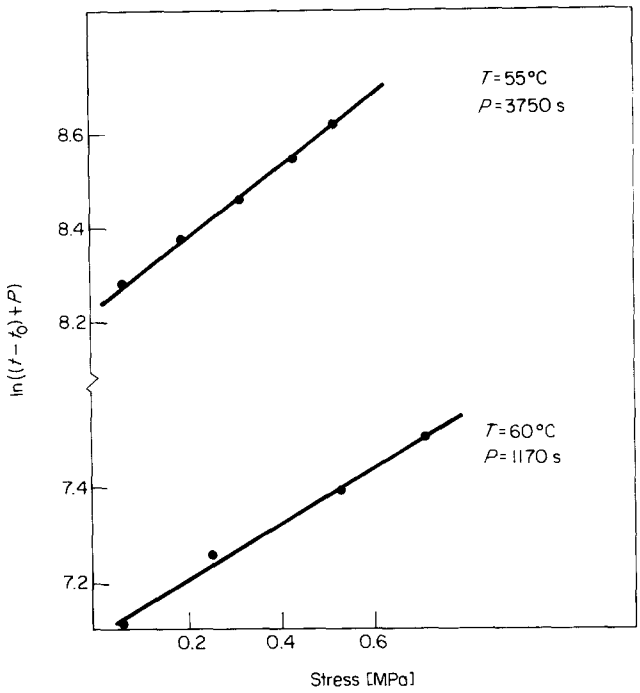

Figure 11 Plots of $\ln(t+P)$ vs. σ for polycarbonate samples

Table 2 Values of activation energy and activation volume in glassy polycarbonate determined by various mechanical tests

Test	Ref.	Activation energy (kcal mol^{-1})	Activation volume (Å^3)
Delayed yielding	8	72	3580
Yielding at constant strain rate	9	73.9	11770
	10	75.5	3385
Shrinkage force	This paper	46	~3000

$$K_{AB} = A\exp\left(-\frac{\Delta G}{RT}\right)\exp\left(-\frac{\sigma V}{kT}\right) \qquad (11)$$

Assuming that $n_b \ll 1$, the solution of equation (8) with K_{AB} given by equation (11) leads to

$$\ln(t+P) = \frac{\sigma V}{kT} + \ln P \qquad (12)$$

where P is a constant. This equation can be used for determination of the activation volume when $\ln(t+P)$ is plotted as a function of σ. Examples of such plots for polycarbonate are shown in *Figure 11* and the activation volumes determined are

$V = 3.3 \times 10^3$ Å^3 at 55°C,

$V = 2.8 \times 10^3$ Å^3 at 60°C,

$V = 2.4 \times 10^3$ Å^3 at 65°C.

The values of activation energy and activation volume obtained for polycarbonate are comparable with those reported by other authors although they were determined for other mechanical processes in glassy polycarbonate. The two sets of values are compared in *Table 2*.

CONCLUSIONS

The agreement obtained between the observed time dependences of shrinkage forces and the time dependences predicted by initial stages of the transition described by the four state model as well as the reasonable values of activation energy and activation volume obtained from this comparison can be regarded as further support for the model introduced in our former paper for the description of thermally stimulated shrinkage forces. The observed induction time of the appearance of shrinkage forces after a temperature jump is, however, not predicted by the model and thus requires further study.

REFERENCES

1 Cleereman, K. J., Karam, K. J. and Williams, J. L. *Mod. Plast.* 1953, **30**, 119
2 Andrews, R. D. *J. Appl. Phys.* 1955, **26**, 1061
3 Tanabe, Y. and Kanetsuna, H. *Polymer* 1979, **20**, 1121
4 Pakula, T. and Trznadel, M., to be published
5 Argon, A. S. and Bessonov, M. I. *Polym. Eng. Sci.* 1977, **17**, 174
6 Janowski, W. 'Mathematics', PWN, Warsaw, 1968
7 Nobbs, J. H., Bower, D. I. and Ward, I. N. *Polymer* 1976, **17**, 25
8 Narisawa, I., Ishikawa, M., Ogawa, N. *Rep. Prog. Polym. Phys. Jpn.* 1978, **2**, 227
9 Brady, T. E. and Yeh, G. S. *J. Appl. Phys.* 1971, **36**, 3057
10 Bauwens-Crowet, C., Bauwens, J. C. and Homes, G. *J. Polym. Sci. A-2* 1965, **7**, 735